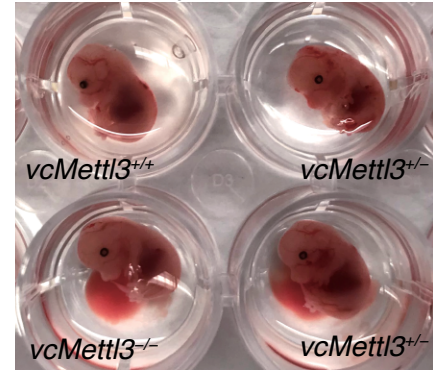
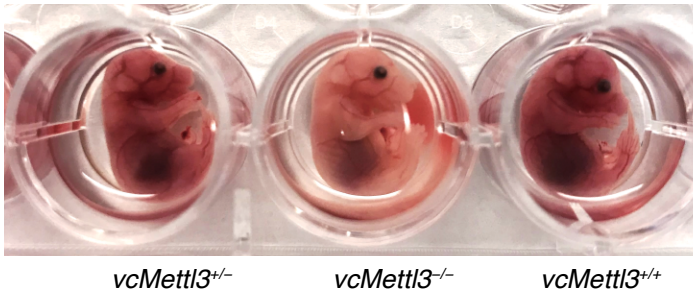


**A**
 $Vav-Cre^+ -Mettl3^{fl/wt} \times Vav-Cre^- -Mettl3^{fl/fl}$ 

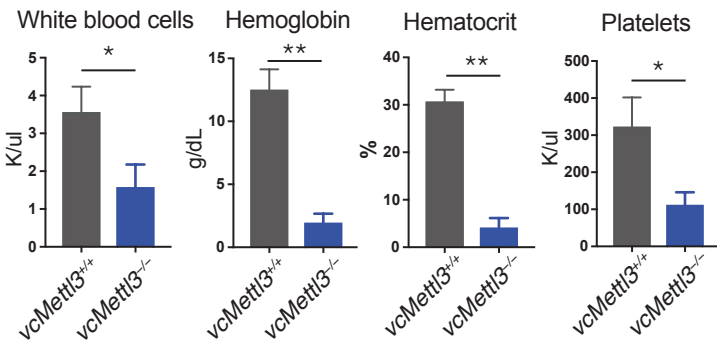
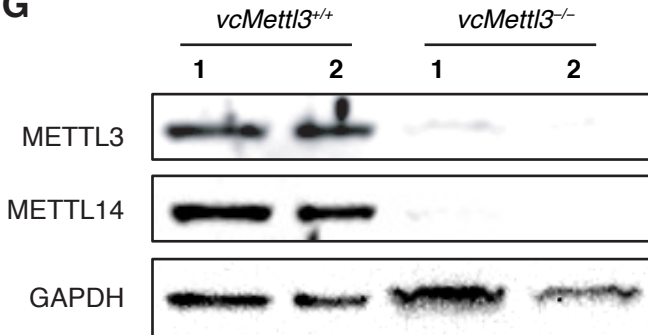
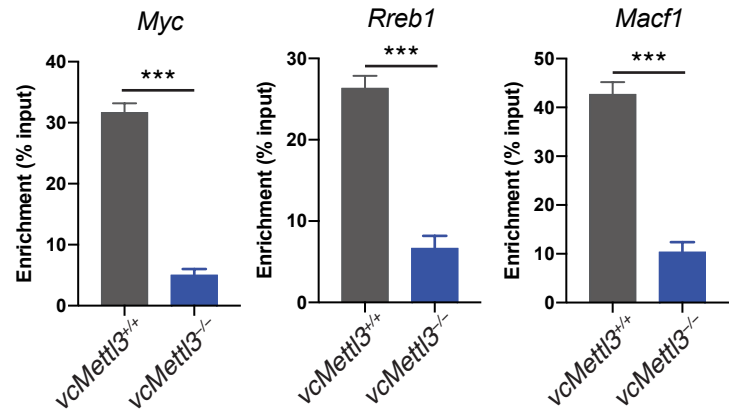
Stage	Litters	<i>vcMettl3</i> <sup>+/+</sup>	<i>vcMettl3</i> <sup>+/-</sup>	<i>vcMettl3</i> <sup>-/-</sup>	Expected <i>vcMettl3</i> <sup>-/-</sup>
E12.5	3	13	4	7	6
E14.5	11	45	29	31	26.25
E16.5	4	21	6	8	8.75
Birth	3	12	7	4	5.75
P10	6	30	17	0	11.75

**B** E14.5 embryos**C**

E16.5 embryos

**D**

Newborn

**E****F***vcMettl3*<sup>+/+</sup> bone Marrow      *vcMettl3*<sup>-/-</sup> bone Marrow**G****H****I**

<i>Vav-Cre</i>						+	-	
<i>Mettl3</i>	+/+					+/+	fl/+	H <sub>2</sub> O
	Kidney	Liver	Lung	Skin	Blood	WT	Het	

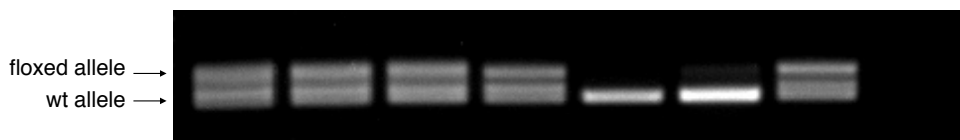


**Figure S1. Vav-Cre mediated *Mettl3* deletion results in bone marrow failure and early demise after birth, related to Figure 1**

(A) Mendelian ratio at the indicated stages. *vcMettl3*<sup>-/-</sup> were expected to be 1/4 of the total mice.

(B-D) Representative photograph of *vcMettl3*<sup>+/+</sup> and *vcMettl3*<sup>-/-</sup> embryos at E14.5 (B), E16.5 (C), and newborns (D).

(E) Peripheral blood counts of *vcMettl3*<sup>+/+</sup> and *vcMettl3*<sup>-/-</sup> newborn mice (n=3 biological replicates per group).

(F) Histology of *vcMettl3*<sup>+/+</sup> and *vcMettl3*<sup>-/-</sup> bone marrow in femur. H&E. Scale bar 100 μm.

(G) Western blot of METTL3 and METTL14 in *vcMettl3*<sup>+/+</sup> and *vcMettl3*<sup>-/-</sup> fetal livers.

(H) Determination of the m<sup>6</sup>A depletion on m<sup>6</sup>A enriched transcripts by m<sup>6</sup>A-RIP-PCR (n=3 biological replicates per group).

(I) Determination of Vav-Cre specificity in hematopoietic system by genotyping of different tissues.

Data are represented as mean ± SEM, and representative of at least three independent experiments; The *P* values were calculated using two-tailed Student's *t* test. \* *p*<0.05, \*\* *p*<0.01, \*\*\* *p*<0.001.

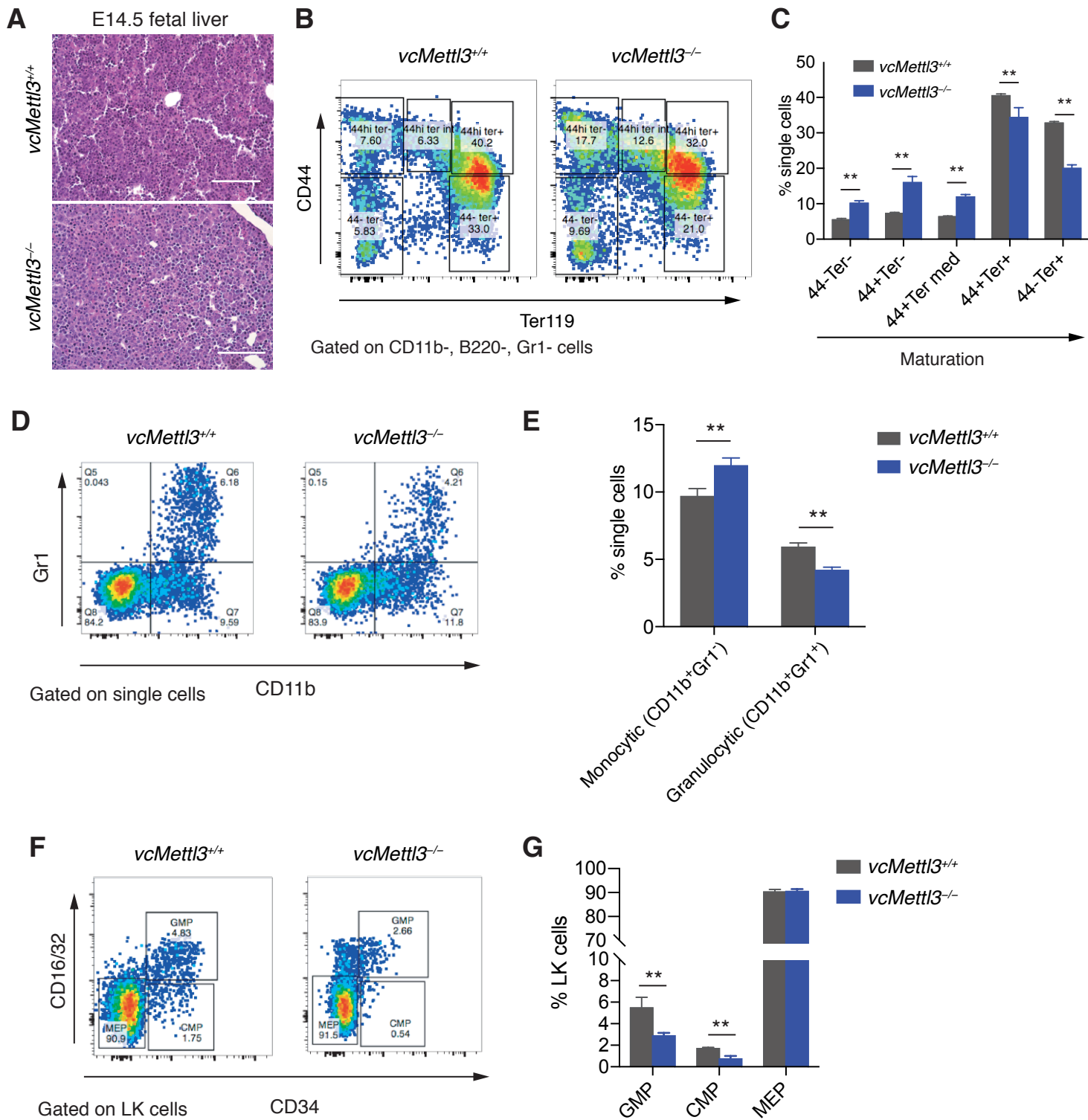


**Figure S2. *vcMettl3*<sup>-/-</sup> fetal liver cells have defective progenitor differentiation and maturation potentials, related to Figure 2**

(A) Histology of *vcMettl3*<sup>+/+</sup> and *vcMettl3*<sup>-/-</sup> E14.5 fetal livers. Scale bar, 100  $\mu$ m.

(B, C) Flow-cytometric evaluation of erythroid differentiation in E14.5 fetal livers, quantified in (C) (n=3 biological replicates per group).

(D, E) Flow-cytometric evaluation of myeloid differentiation in E14.5 fetal livers, quantified in (E) (n=3 biological replicates per group).

(F, G) Determination of myeloid progenitor distribution, GMP (CD16/32<sup>+</sup>CD34<sup>+</sup> LK), CMP (CD16/32<sup>-</sup>CD34<sup>+</sup> LK), and MEP (CD16/32<sup>-</sup>CD34<sup>-</sup> LK) in E14.5 fetal livers (n=3 biological replicates per group).

Data are represented as mean  $\pm$  SEM, representative of at least three independent experiments; The *P* values were calculated using two-way ANOVA. \*\* *p*<0.01.

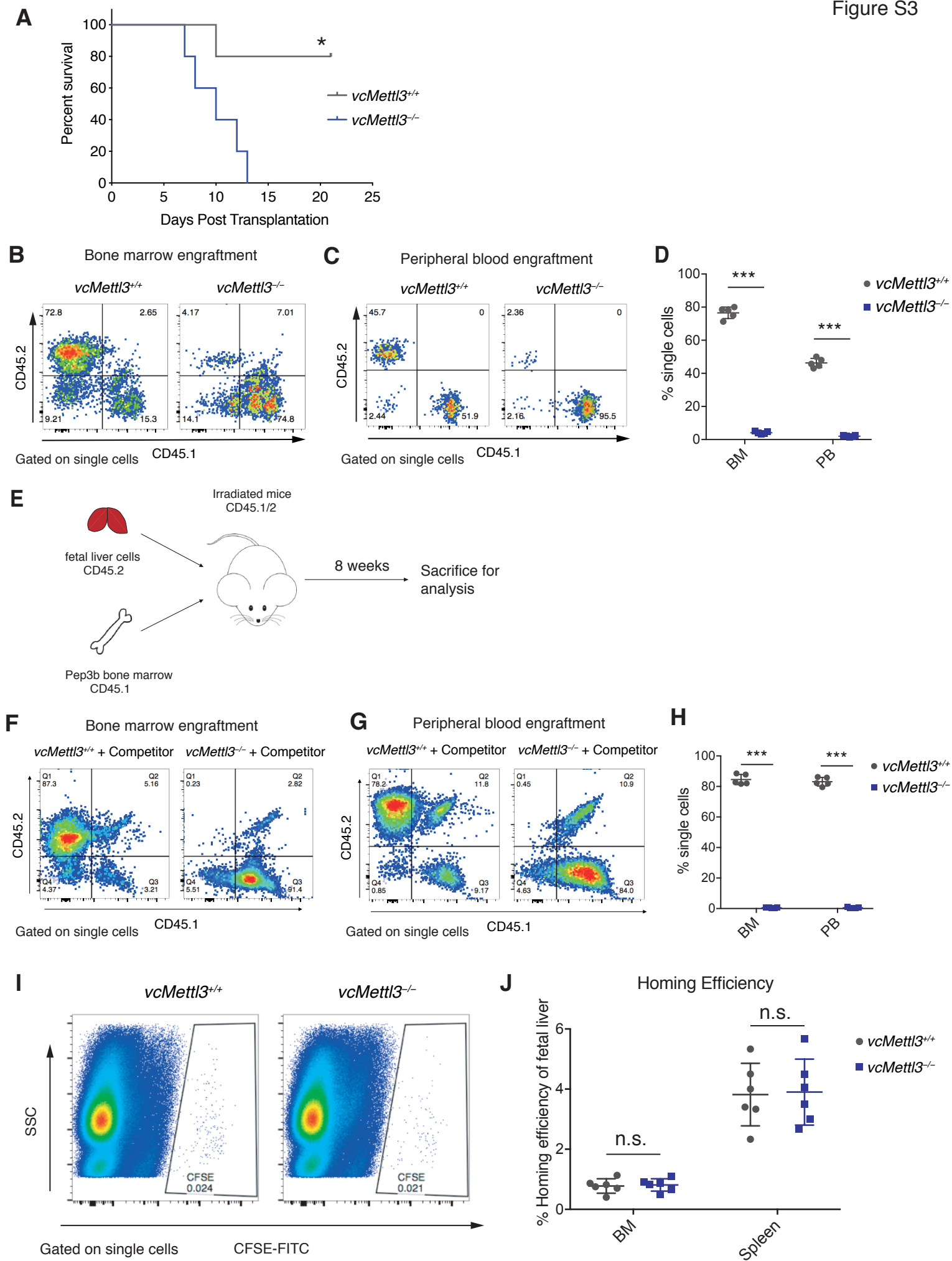


**Figure S3. *vcMettl3*<sup>-/-</sup> fetal liver HSPCs fail to repopulate lethally irradiated recipients, related to Figure 2**

(A) Kaplan-Meier survival curves of recipient mice transplanted with *vcMettl3*<sup>+/+</sup> and *vcMettl3*<sup>-/-</sup> fetal liver cells (n=5 mice per group).

(B-D) Contribution of CD45.2<sup>+</sup> *vcMettl3*<sup>+/+</sup> and *vcMettl3*<sup>-/-</sup> cells in lethally irradiated congenic CD45.1<sup>+</sup> Pep3b recipient mouse bone marrow (B) and peripheral blood (C) 8 days after transplantation, quantified in (D) (n=5 mice per group).

(E) Scheme of competitive transplantation of *vcMettl3*<sup>+/+</sup> and *vcMettl3*<sup>-/-</sup> fetal liver cells against Pep3b bone marrow into lethally irradiated recipient mice.

(F-H) Contribution of CD45.2<sup>+</sup> *vcMettl3*<sup>+/+</sup> and *vcMettl3*<sup>-/-</sup> fetal liver cells in competition with CD45.1<sup>+</sup> bone marrow cells in lethally irradiated congenic CD45.1/2 recipient mouse bone marrow (F) and peripheral blood (G), quantified in (H) (n=5 mice per group).

(I, J) Flow-cytometric detection of homing of CFSE labeled fetal liver hematopoietic cells in recipient bone marrow (I, J) and spleen (J) (n=6 mice per group).

Data are represented as mean ± SEM, and representative of at least three independent experiments; The *P* value in (A) was calculated using log-rank test. \**p* < 0.05. The *P* values in (D), (H) and (J) were calculated using two-tailed Student's *t* test; n.s., not statistically significant; \*\*\* *p*<0.001.

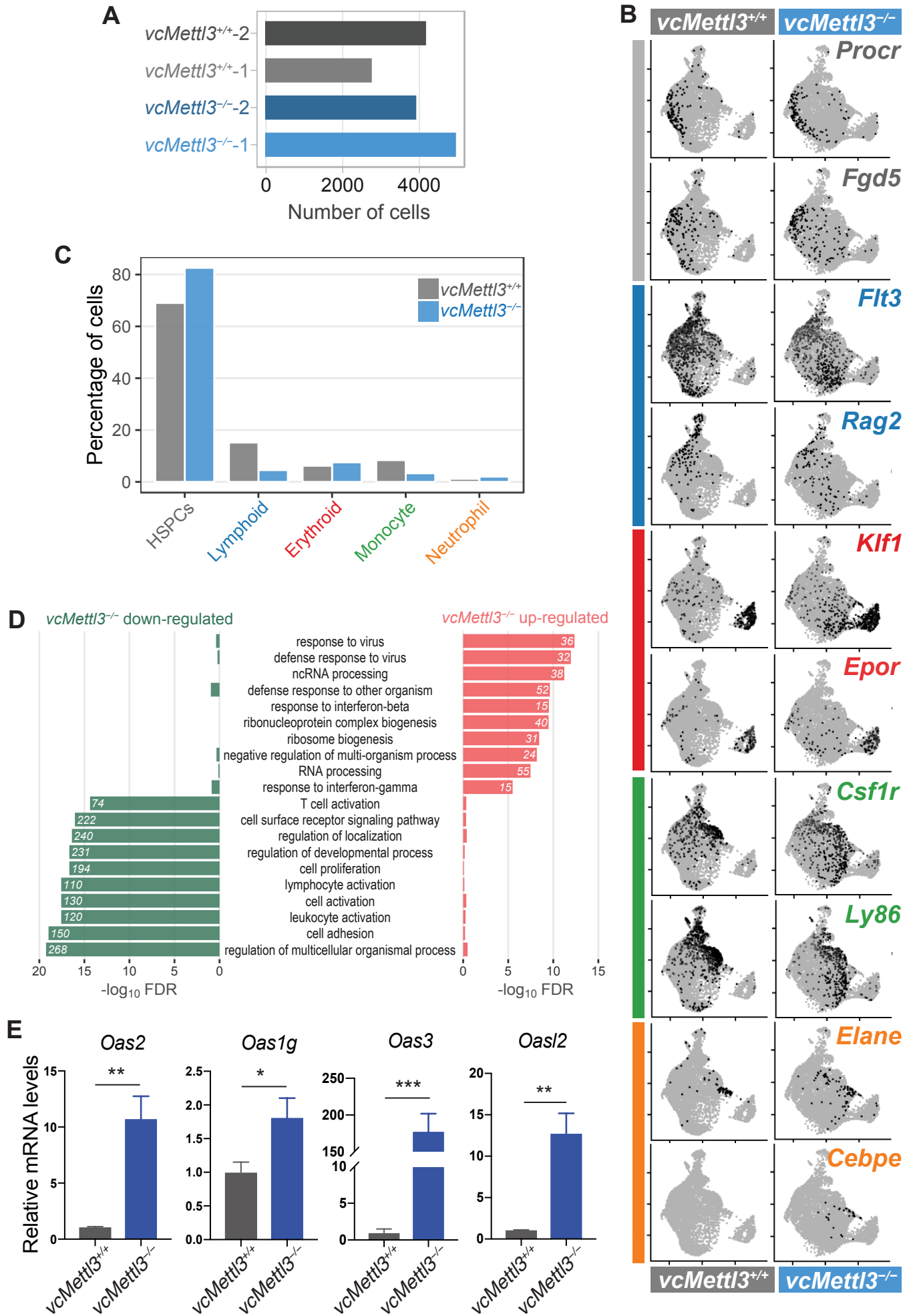


**Figure S4. Gene expression changes upon *Mettl3* deletion in fetal liver LSK cells, related to Figure 3**

(A) Number of unique LSK cells with more than 500 quantified genes, used for further single cell RNA-Seq (scRNA-seq) analysis. scRNA-Seq was performed in duplicate.

(B) Expression of marker genes used for the assignation of cell clusters to hematopoietic populations and differentiation entry points: HSPCs (grey), lymphoid (blue), erythroid (red), monocyte (green), neutrophil (orange). Marker expression is plotted on the UMAP representation of *vcMettl3*<sup>+/+</sup> and *vcMettl3*<sup>-/-</sup> LSK cells (light grey: low expression, black: maximum expression). Two markers for each clusters are shown.

(C) Percentage of *vcMettl3*<sup>+/+</sup> and *vcMettl3*<sup>-/-</sup> LSK cells composing each cluster identified by scRNA-Seq.

(D) Gene ontology (GO) enrichment analysis of genes significantly upregulated or significantly down-regulated in bulk RNA-seq of *vcMettl3*<sup>-/-</sup> LSK compared to *vcMettl3*<sup>+/+</sup> LSK cells. The number of differentially expressed genes within each category is displayed.

(E) Q-RT-PCR determination of expression of members of the OAS family of genes in *vcMettl3*<sup>-/-</sup> versus *vcMettl3*<sup>+/+</sup> E14.5 fetal liver cells (n=3 biological replicates per group). Data are representative of three independent experiments.

Data are represented as mean  $\pm$  SEM; The *P* value was calculated using two-tailed Student's *t* test. \*  $p < 0.05$ , \*\*  $p < 0.01$ , \*\*\*  $p < 0.001$ .



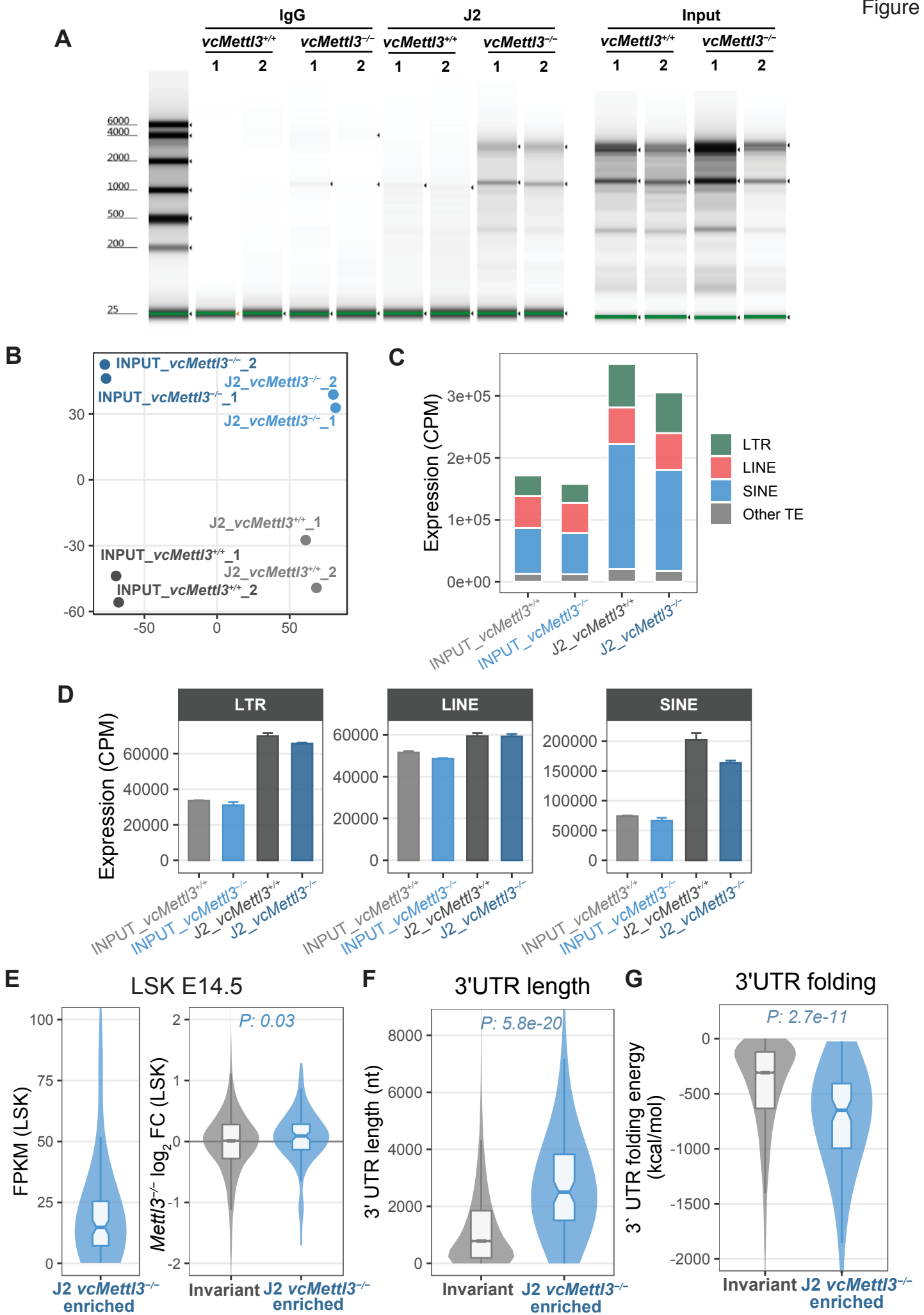


**Figure S5. J2-RIP specifically isolates dsRNAs in fetal livers, related to Figure 5**

(A) RNA chip analysis of J2-RIP, IgG-RIP and input RNA of *vcMettl3<sup>+/+</sup>* and *vcMettl3<sup>-/-</sup>* fetal livers.

(B) Multidimensional Scaling plot of samples from the J2-RIP-Seq experiment (*vcMettl3<sup>+/+</sup>* and *vcMettl3<sup>-/-</sup>*, J2 and INPUT), based on gene-specific signals.

(C) Average expression levels of transposable element classes in *vcMettl3<sup>+/+</sup>* and *vcMettl3<sup>-/-</sup>* fetal livers in J2-RIP and INPUT samples. CPM: Counts Per Million. LTR: Long Terminal Repeat. LINE: Long INterspersed Elements. SINE: Short INterspersed Elements.

(D) Expression levels of specific retrotransposon classes (LTR, LINE, SINE) in J2-RIP samples (n=2 biological replicates per group). CPM: Counts Per Million.

(E) Distribution of the expression levels (left) and *vcMettl3<sup>-/-</sup>* fold changes (right) of *vcMettl3<sup>-/-</sup>* J2-RIP enriched genes in LSK cells. FPKM: Fragments Per Kilobase of transcript per Million.

(F) Distribution of the 3'UTR length of *vcMettl3<sup>-/-</sup>* J2-RIP enriched genes compared with invariant genes.

(G) Distribution of the predicted 3'UTR folding energy of *vcMettl3<sup>-/-</sup>* J2-RIP enriched genes compared with invariant genes.

The *P* values in (E, F, G) were calculated using two-tailed Wilcoxon rank-sum test.

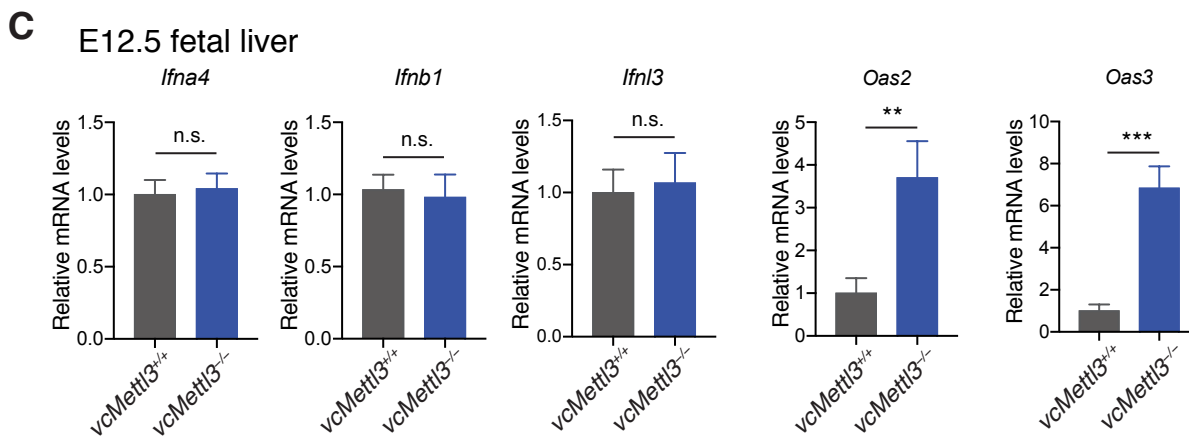
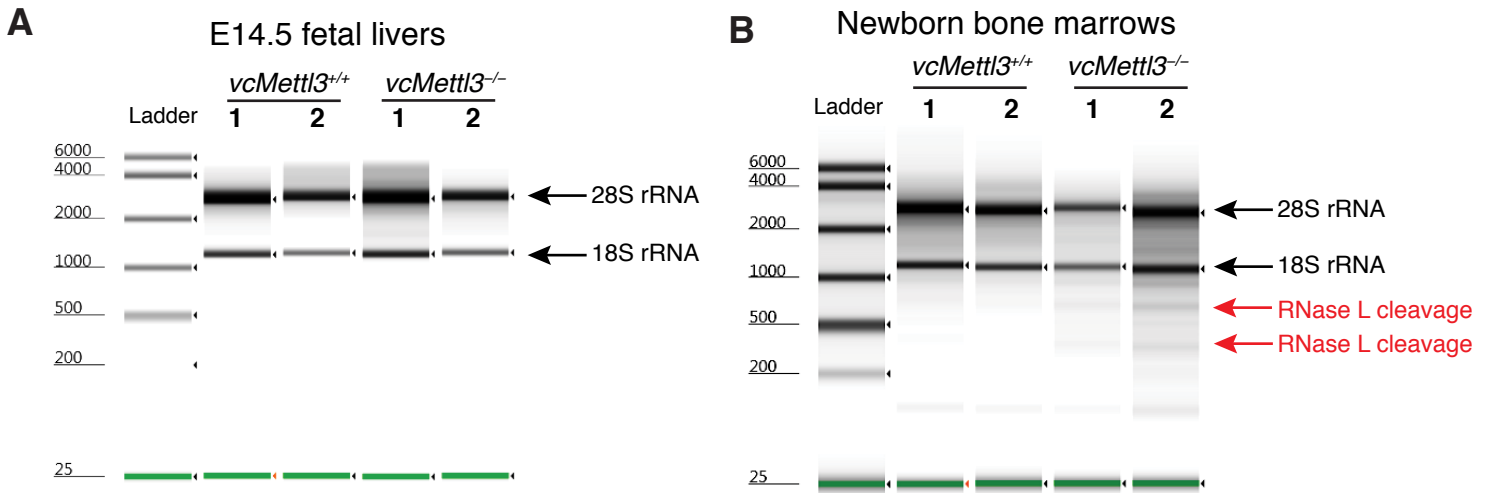


**Figure S6. Innate immune response is activated in *vcMettl3*<sup>-/-</sup> fetal livers, related to Figure 6**

(A) RNA chip analysis for cleavage of ribosomal RNA (rRNA) by RNase L in E14.5 fetal livers.

(B) RNA chip analysis for cleavage of rRNA by RNase L in bone marrows of newborn mice.

(C) Determination of IFN and OAS family expression levels at E12.5 fetal livers (n=3 biological replicates per group).

Data are represented as mean  $\pm$  SEM, and representative of three independent experiments;

The *P* values were calculated using two-tailed Student's *t* test. n.s. not statistically significant, \*\*

$p < 0.01$ , \*\*\*  $p < 0.001$ .

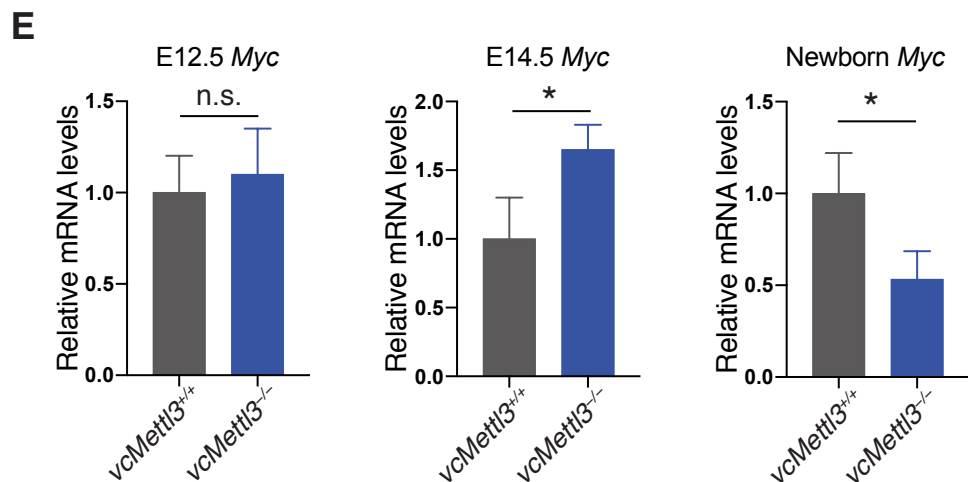
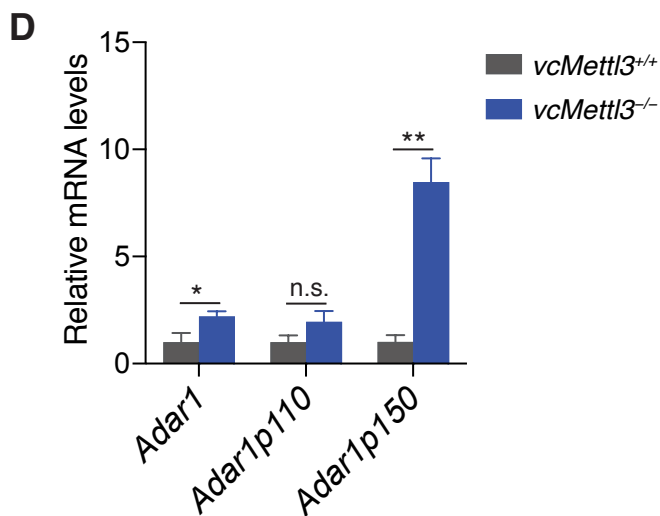
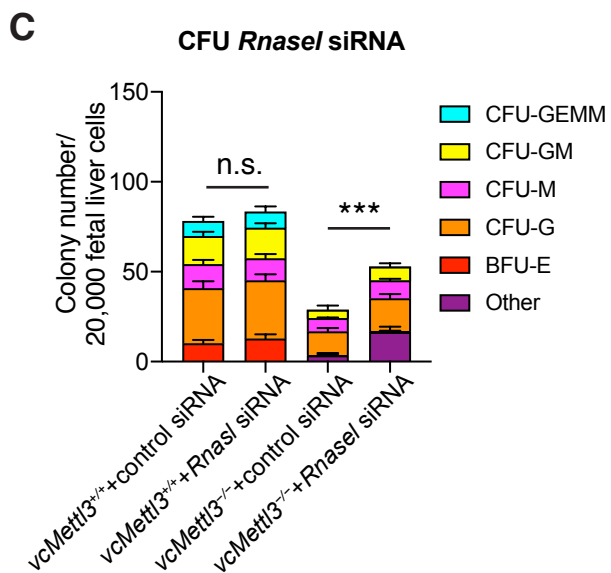
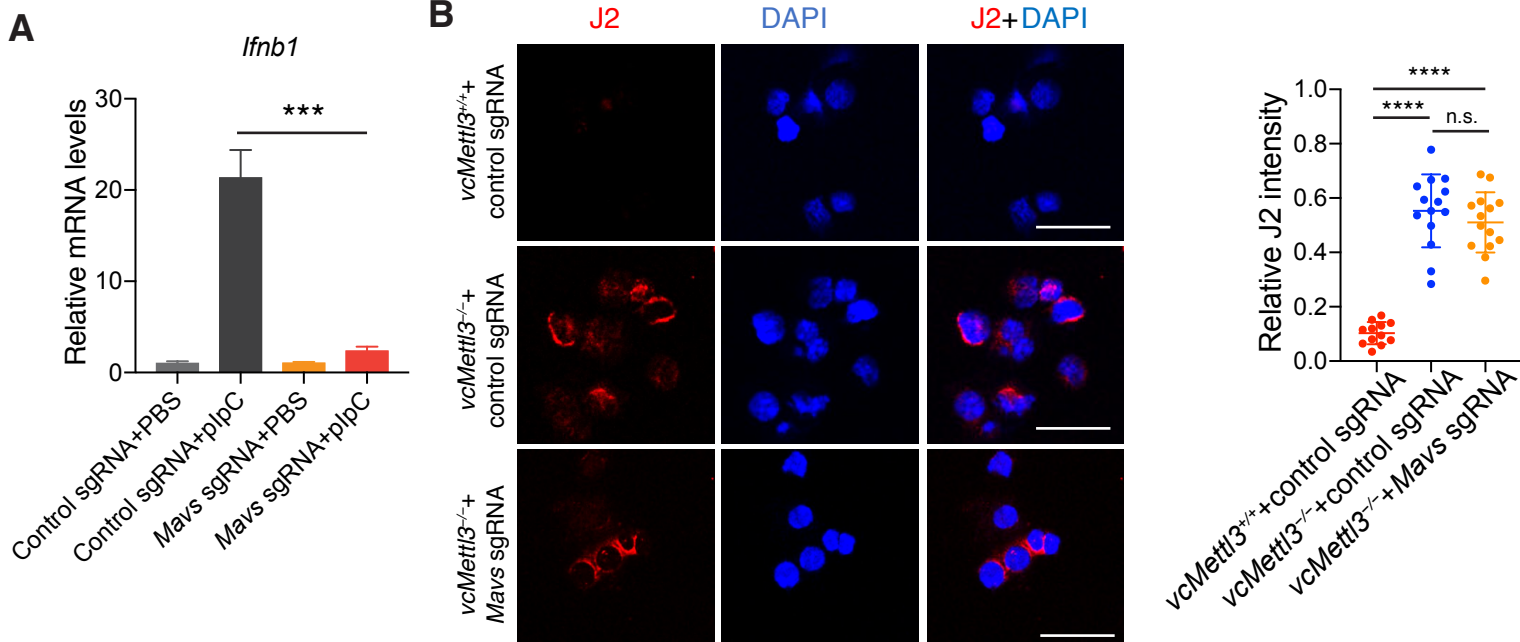


**Figure S7. Inhibition of innate immune response partially rescues the hematopoietic failure caused by *Mettl3* deletion, related to Figure 7**

(A) Determination of *Ifnb1* expression in *vcMettl3*<sup>-/-</sup> cells after deletion of *Mavs* under the treatment of plpC (n=3 biological replicates per group).

(B) Measurement of dsRNA in lineage depleted fetal liver cells with deletion of *Mavs* by J2 immunofluorescent staining (*vcMettl3*<sup>+/+</sup>+control sgRNA n=12, *vcMettl3*<sup>-/-</sup>+control sgRNA n=14, *vcMettl3*<sup>-/-</sup>+*Mavs* sgRNA n=14).

(C) Colony formation unit (CFU) of E14.5 fetal liver cells transfected with control siRNA or *Rnase1* siRNA (n=3 biological replicates per group).

(D) Time course of *c-Myc* expression levels in fetal livers at E12.5, E14.5 and bone marrows of newborn mice (n=3 biological replicates per group).

(E) Determination of the expression levels of *Adar1* and its isoforms in fetal livers by Q-RT-PCR (n=3 biological replicates per group).

Data are represented as mean ± SEM, and representative of three independent experiments; The *P* values were calculated using two-tailed Student's *t* test. n.s. not statistically significant, \*  $p < 0.05$ , \*\*  $p < 0.01$ , \*\*\*  $p < 0.001$ , \*\*\*\*  $p < 0.0001$ .